AIP Applied Physics Letters

Fabrication of Si 1 − x Ge x alloy nanowire field-effect transistors

Cheol-Joo Kim, Jee-Eun Yang, Hyun-Seung Lee, Hyun M. Jang, Moon-Ho Jo, Won-Hwa Park, Zee Hwan Kim, and Sunglyul Maeng

Citation: Applied Physics Letters **91**, 033104 (2007); doi: 10.1063/1.2753722
View online: http://dx.doi.org/10.1063/1.2753722
View Table of Contents: http://scitation.aip.org/content/aip/journal/apl/91/3?ver=pdfcov
Published by the AIP Publishing

Fabrication of $Si_{1-x}Ge_x$ alloy nanowire field-effect transistors

Cheol-Joo Kim, Jee-Eun Yang, Hyun-Seung Lee, Hyun M. Jang, and Moon-Ho Jo[a)]
Department of Materials Science and Engineering, Pohang University of Science and Technology (POSTECH), San 31, Hyoja-Dong, Nam Gu, Pohang, Gyungbuk 790-784 Korea

Won-Hwa Park and Zee Hwan Kim
Department of Chemistry, Korea University, Anam-Dong, Seongbuk-Gu, Seoul 136-701, Korea

Sunglyul Maeng
Cambridge-ETRI Joint Research Centre, Electronics and Telecommunications Research Institute, 161 Gajeong-Dong, Yuseong-gu, Daejeon 305-700, Korea

(Received 26 April 2007; accepted 10 June 2007; published online 17 July 2007)

The authors present the demonstration of nanowire field-effect transistors incorporating group IV alloy nanowires, $Si_{1-x}Ge_x$. Single-crystalline $Si_{1-x}Ge_x$ alloy nanowires were grown by a Au catalyst-assisted chemical vapor synthesis using SiH_4 and GeH_4 precursors, and the alloy composition was reproducibly controlled in the whole composition range by controlling the kinetics of catalytic decomposition of precursors. Complementary *in situ* doping of $Si_{1-x}Ge_x$ nanowires was achieved by PH_3 and B_2H_6 incorporation during the synthesis for *n*- and *p*-type field-effect transistors. The availability of both *n*- and *p*-type $Si_{1-x}Ge_x$ nanowire circuit components suggests implications for group IV semiconductor nanowire electronics and optoelectronics. © *2007 American Institute of Physics*. [DOI: 10.1063/1.2753722]

Group IV semiconductor alloys offer a continuously variable system of crystal lattices and energy band gaps, leading to interesting applications into electronics and optoelectronics.[1] For example, $Si_{1-x}Ge_x$ thin films offer a lattice-engineered platform for strained Si carrier channels with enhanced carrier mobility in $Si/Si_{1-x}Ge_x$ heteroepitaxial structures in high speed electronics, and they also serve as long wavelength photodetectors in optical communications.[2,3] More interestingly nanocrystalline $Si_{1-x}Ge_x$ provides challenging opportunities for efficient light emitters/detectors in Si optoelectronics, since it can potentially allow enhanced emission and detection of the photons in the wide energy band gap, i.e., the wavelength range of optical fiber communication.[4,5] One-dimensional $Si_{1-x}Ge_x$ nanocrystals, in this sense, can serve as attractive test beds to investigate the interplay between electronic charge transport and light emission/detection processes, because one can integrate electrical and optical components within the individual nanowires.[6,7] Here, to this end, we report the synthesis and characterization of *n*-type and *p*-type $Si_{1-x}Ge_x$ nanowires as elemental nanowire device blocks in electronic and optical circuits. Specifically, single-crystalline $Si_{1-x}Ge_x$ nanowires in the whole range of $0 \leqslant x \leqslant 1$ were synthesized by Au catalysts-assisted chemical vapor depositions (CVDs), and were identified as Si:Ge random alloys by micro-Raman scattering and electron microscopy studies within the instrumental limits. Single-crystalline $Si_{1-x}Ge_x$ nanowires were for the first time *in situ* doped with PH_3 and B_2H_6 as *n* and *p* dopants during the CVD growth, and we then demonstrated fabrication of *n*-type and *p*-type $Si_{1-x}Ge_x$ nanowire field-effect transistors. We argue that the availability of both *n*- and *p*-type $Si_{1-x}Ge_x$ nanowire components in this study suggests implications for group IV semiconductor nanowire electronics and optoelectronics.

Single-crystalline $Si_{1-x}Ge_x$ nanowires were grown by the Au catalyst-assisted chemical vapor process.[4,8–10] The Au catalysts of the nanometer scale were prepared by dispersion of colloidal Au particles of 10–50 nm in diameter on SiO_2/Si (100), and are subsequently loaded in a quartz tube furnace. Then the nanowire crystal growth was carried out under a constant flow of independent SiH_4 and GeH_4 precursors (specifically, 10% of SiH_4 and GeH_4 premixed in H_2) at given temperatures. Figures 1(a) and 1(b) show representative scanning and transmission electron microscopy images of individual $Si_{1-x}Ge_x$ nanowires. The presence of Au catalysts at the front tip of the nanowires, as in the inset of Fig. 1(a), suggests that the growth is governed by vapor-liquid-solid mechanism.[11,12] We also confirmed that the nanowires are single crystalline with the same crystal orientation along the entire nanowire length, as in the inset of Fig. 1(b), although the crystal orientation with respect to the nanowire axis usually varies for the nanowires of different diameters.[13] The relative composition of Si and Ge in $Si_{1-x}Ge_x$ nanowires is determined from energy dispersive x-ray (EDX) spectra probed on individual nanowires by the convergent electron beam in TEM. We quantitatively determined the relative composition using the *k* factor of Si K_α and Ge K_α radiations in the EDX spectra, as representatively shown for $Si_{0.7}Ge_{0.3}$ nanowires in Fig. 1(c). The Si:Ge composition is variant only within 5% variation along the nanowire and this finding suggests appropriate alloying of Si and Ge within the nanowires without forming any obvious long range ordering. Figure 2 illustrates the relationship between the Ge precursor pressure ratio in the reactor during the CVD growth and the Ge content in the nanowires, and notably the reaction requires much less GeH_4 precursor for the corresponding compositions, due to the much faster thermal decomposition kinetics than that of SiH_4.[4,10] This faster thermal decomposition rate of GeH_4 promotes homogeneous decomposition (radial growth) over catalytic decomposition (axial growth), and typically manifests itself as the tapered shape.[8,10] Thus, in this study, we

[a)]Electronic mail: mhjo@postech.ac.kr

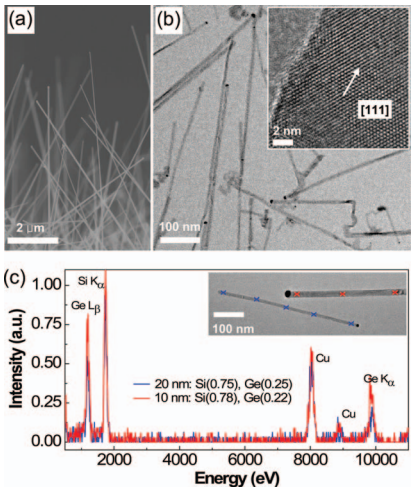

FIG. 1. (Color) (a) Scanning electron microscope image of $Si_{0.7}Ge_{0.3}$ nanowires (b) Transmission electron microscope images of individual $Si_{0.7}Ge_{0.3}$ nanowires. Inset is a high-resolution image from the middle section of a nanowire, showing the crystal orientation along the nanowire length is [111]. (c) Energy dispersive x-ray (EDX) spectra collected from individual $Si_{0.3}Ge_{0.7}$ nanowires of 10 and 20 nm diameter. Inset is a TEM image of $Si_{0.3}Ge_{0.7}$ nanowires of 10 and 20 nm diameter, and the EDX spectra were collected from different positions within the individual nanowires as marked by x.

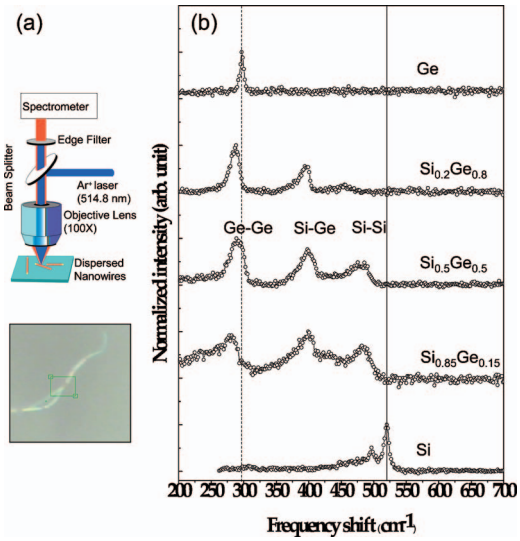

FIG. 3. (Color) (a) Schematics of micro-Raman scattering setup in this study. A typical bright field optical microscope image of individual $Si_{1-x}Ge_x$ nanowire dispersed on glass substrates is shown at the right, where the sides of a square are 30 μm. (b) Micro-Raman scattering spectra of individual $Si_{1-x}Ge_x$ nanowires of 50 nm in diameter for various Ge compositions. Two vertical lines (solid and dotted) define the peak positions of Si–Si and Ge–Ge from the pure Si and Ge nanowires.

have paid particular attention in order to avoid the radial growth, and found that H_2 introduction into the reactor during the growth effectively suppressed the radial growth.[4,8,14] There is usually a finite diameter distribution due to different sizes of Au catalysts formed at the nanowires growth conditions, and we have found a general tendency that the Ge content is smaller in thinner $Si_{1-x}Ge_x$ nanowires: at almost all growth conditions we observed size-dependent composition variation by up to 10%, particularly when the diameter varies below 20 nm—see also Fig. 1(c). We are under further investigation on this observation based on thermodynamic calculations.

Figure 3 shows a series of Raman scattering spectra of individual $Si_{1-x}Ge_x$ nanowires for various Ge compositions, collected from the Ar laser excitation (514.8 nm) whose spot size is ~500 nm in diameter, as schematically seen in Fig. 3(a). The nanowires were dispersed on glass substrates and the Raman spectra were obtained by subtracting the background signals collected when the laser was focused on the

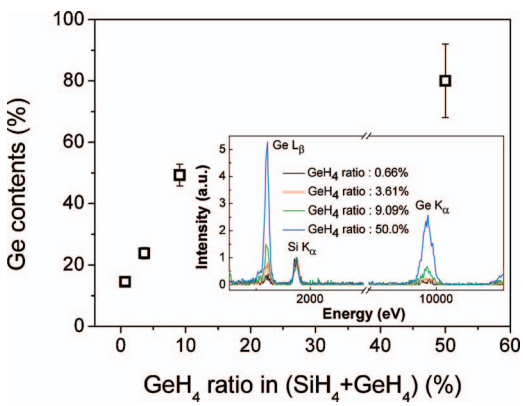

FIG. 2. (Color) Variation in the Ge content in the nanowires of 20 nm in diameter with the relative GeH_4 pressure ratio in the total (SiH_4+GeH_4) pressure. The inset shows the corresponding energy dispersive x-ray spectra in the main panel.

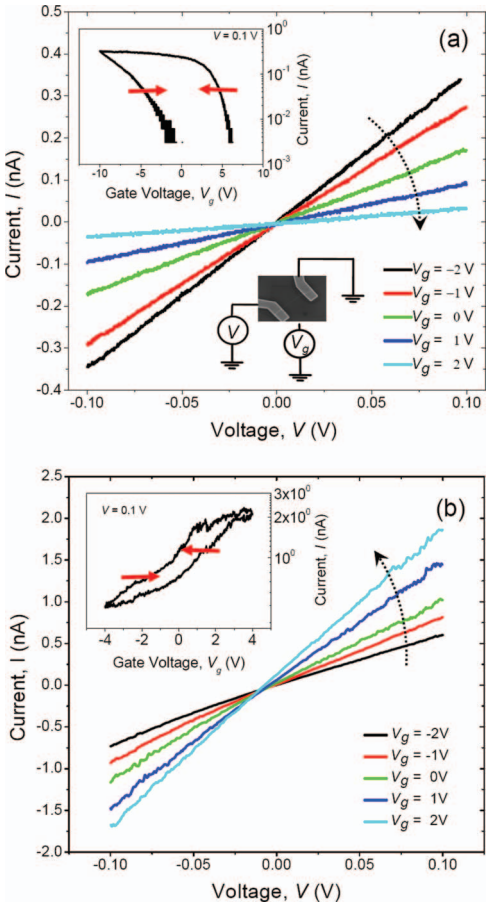

FIG. 4. (Color) Current (I)-voltage (V) characteristics recorded on (a) a 40 nm thick B-doped and (b) a 80 nm thick P-doped $Si_{0.5}Ge_{0.5}$ nanowire at various gate voltages (V_g). The lower inset of (a) is a scanning electron micrograph of a representative nanowire FET along with a simplified measurement scheme. A dotted arrow represents the direction of positively increasing gate voltages. The upper insets are I-V_g at V=0.1 V. The arrows represent the sweep direction of gate voltage.

glass substrates from the signals of the nanowires. There are three major Raman peaks at around 300, 400, and 500 cm^{-1}, and they can be assigned to the optical phonon modes associated with the local Ge–Ge, Si–Ge, and Si–Si vibrations, as similarly characterized on bulk and nano-$Si_{1-x}Ge_x$ crystals in the literature.[15,16] As it is qualitatively expected, with the increasing Ge content from pure Si nanowires, the peak intensity of the Si–Ge and Ge–Ge peaks increases, and only the Ge–Ge vibration peak is present for pure Ge nanowires. It is notable that in the $Si_{1-x}Ge_x$ alloys the mode frequency of both the Si–Si and Ge–Ge peaks shift to lower frequencies accompanied by the peak broadening, compared to those of the pure Si and Ge nanowires. It was reported that in randomly alloyed $Si_{1-x}Ge_x$ crystals, i.e., Si and Ge are substitutionally introduced in the lattice of each other, the localized mode vibrations occurs at lower frequencies with some degrees of mode inhomogeneity than those in perfect crystals.[15,16] Our observations are consistent with the previous reports, and thus further support the fact that Si and Ge essentially form compositionally random alloys within the individual nanowires without any obvious long range ordering of Si or Ge, as discussed above.

Figure 4 shows the current (I)-voltage (V) characteristics of p-type and n-type $Si_{0.5}Ge_{0.5}$ nanowire field-effect transistors at various gate voltages (V_g) in this study. These $Si_{0.5}Ge_{0.5}$ nanowires were *in situ* doped with PH_3 and B_2H_6 at the SiH_4:GeH_4:(PH_3 or B_2H_6) gas pressure ratio of $10:1:2\times10^{-3}$, from which the nanowire transistors are fabricated on SiO_2/degenerated Si substrates by e-beam lithography and the Ni/Au (30/100 nm) lift-off, as seen in the lower inset of Fig. 3(a). Electrical transport measurements were taken on individual nanowire field-effect transistors (FETs) using a home-built system with a minimum noise level of $\leqslant$2 pA. As in the lower inset of Fig. 4(a), the bias voltage (V) was applied to the source electrode with respect to the drain electrode, and the gate voltage was applied through degenerated Si substrates across SiO_2 insulators to vary the electrostatic potential of the $Si_{1-x}Ge_x$ nanowire channels of 40 nm in diameter. Figure 4(a) shows V_g-dependent I-V characteristics measured on a B-doped $Si_{1-x}Ge_x$ nanowire. The I-V curves are linear within the voltage range applied, from which the resistivity of this B-doped $Si_{1-x}Ge_x$ nanowire is calculated to be 1.74×10^{1} Ω cm at $V_g=0$ V. Notably, the currents were suppressed with positively increasing of V_g, as represented by an arrow, and this gate voltage dependence is a typical character of p-type field-effect transistor. This behavior is also shown in the upper inset, where the current varies with applied gate voltage (I-V_g) at a constant V of 0.1 V. Typically we observed hysteretic I-V_g, as we change the directions of gate voltage sweep and it is presumably due to trap charges existing at the nanowire/SiO_2 interface and in the oxide. In the same manners, seen from I-V-V_g and I-V_g data in Fig. 4(b), we identified the typical n-type field-effect transistor character from P-doped $Si_{1-x}Ge_x$ nanowires (of 80 nm in diameter) whose resistivity is calculated to be 9.27 Ω cm at $V_g=0$ V. The carrier mobilities are estimated, using an assumption regarding the nanowire as a cylindrical capacitor, to be 6.07×10^{-1} and 2.09 $cm^2/V\,s$ for B-doped and P-doped $Si_{1-x}Ge_x$ nanowire FETs, respectively. We consider that these values are much smaller than the reported values from pure Si or Ge nanowires,[17,18] and yet can be enhanced by an optimal design of FET structures, for example, by appropriate surface passivation of thinner $Si_{1-x}Ge_x$ nanowire channels with high-k dielectrics as gate insulators. Here we can only comment that we have for the first time demonstrated the appropriate FET operations based on n-type and p-type $Si_{1-x}Ge_x$ nanowires.

In summary we have synthesized single-crystalline $Si_{1-x}Ge_x$ alloy nanowires in the whole range of $0\leqslant x\leqslant1$ by the Au catalyst-assisted chemical vapor synthesis, and micro-Raman scattering and electron microscope studies on individual nanowires show that Si and Ge form random alloys within the same crystal structures within the nanowires. We have also incorporated PH_3 and B_2H_6 dopants during the nanowire growth, and fabricated nanowire field-effect transistors based on these nanowires. We have verified that the appropriate n- and p-type FET operations can be available from these *in situ* P-doped and B-doped $Si_{1-x}Ge_x$ nanowire components.

This work was financially supported by MOST-AFOSR NBIT Program 2007, Nano R&D program 2007, the Basic Research Program (R01–2005–000–10711–0) through KOSEF funded by the Ministry of Science & Technology, the Korean Research Foundation Grant MOEHRD (KRF-2005-005-J13103), Basic Research Promotion Fund (KRF-2006-311-D00114), Ministry of Information and Communication of Korea (A1100-0602-0101), and POSTECH Core Research Program.

[1] O. Madelung, *In Semiconductors: Data Handbook*, 2nd ed. (Springer, Berlin, 1996), Vol. 2, p. 11.
[2] For a recent review, D. J. Paul, Semicond. Sci. Technol. **19**, R75 (2004).
[3] J. Ouellette, Ind. Phys. **8**, 18 (2002).
[4] Jee-Eun Yang, Chang-Beom Jin, Cheol-Joo Kim, and Moon-Ho Jo, Nano Lett. **6**, 2679 (2006).
[5] H. Takagi, H. Ogawa, Y. Yamazaki, A. Ishizaki, and T. Nakagiri, Appl. Phys. Lett. **56**, 2379 (1990); S. Schuppler, S. L. Friedman, M. A. Marcus, D. L. Adler, Y.-H. Xie, F. M. Ross, T. D. Harris, W. L. Brown, Y. J. Chabal, L. E. Brus, and P. H. Citrin, Phys. Rev. Lett. **72**, 2648 (1994); T. van Buuren, L. N. Dinh, L. L. Chase, W. J. Siekhaus, and L. J. Terminello, *ibid.* **80**, 3803 (1998).
[6] Y. Li, F. Qian, J. Xiang, and C. M. Lieber, Mater. Today **9**, 18 (2006).
[7] O. Hayden, R. Agarwal, and C. M. Lieber, Nat. Mater. **5**, 352 (2006); M. S. Gudiksen, K. N. Maher, L. Ouyang, and H. Park, Nano Lett. **5**, 2257 (2005); H. Pettersson, J. Tragardh, A. I. Persson, L. Landin, D. Hessman, and L. Samuelson, *ibid.* **6**, 229 (2006).
[8] Chang-Beom Jin, Jee-Eun Yang, and Moon-Ho Jo, Appl. Phys. Lett. **88**, 193105 (2006).
[9] X. F. Duan and C. M. Lieber, Adv. Mater. (Weinheim, Ger.) **12**, 298 (2000).
[10] K. K. Lew, L. Pan, E. C. Dickey, and J. M. Redwing, Adv. Mater. (Weinheim, Ger.) **15**, 2073 (2003).
[11] R. S. Wagner and W. C. Eliis, Appl. Phys. Lett. **4**, 89 (1964).
[12] A. M. Morales and C. M. Lieber, Science **279**, 208 (1998).
[13] Y. Wu, Y. Cui, L. Huynh, C. J. Barrelet, D. C. Bell, and C. M. Lieber, Nano Lett. **4**, 433 (2004).
[14] L. J. Lauhon, M. S. Gudiksen, C. L. Wang, and C. M. Lieber, Nature (London) **420**, 57 (2002).
[15] M. I. Alonso and K. Winer, Phys. Rev. B **39**, 10056 (1989); M. Franz, K. F. Dombrowski, H. Rucker, B. Dietrich, and K. Pressel, *ibid.* **59**, 10614 (1999); Z. F. Sui, H. H. Burke, and I. P. Herman, *ibid.* **48**, 2162 (1993).
[16] S. Takeoka, K. Toshikiyo, M. Fujii, S. Hayashi, and K. Yamamoto, Phys. Rev. B **61**, 15988 (2000).
[17] S. L. Wu, Semicond. Sci. Technol. **20**, 559 (2005).
[18] A. B. Greytak, L. J. Lauhon, M. S. Gudiksen, and C. M. Lieber, Appl. Phys. Lett. **84**, 4176 (2004); Y. Cui, Z. H. Zhong, D. L. Wang, and C. M. Lieber, Nano Lett. **3**, 149 (2003); G. F. Zheng, W. Lu, S. Jin, and C. M. Lieber, Adv. Mater. (Weinheim, Ger.) **16**, 1890 (2004); Y. Gu, E. S. Kwak, J. L. Lensch, J. E. Allen, T. W. Odom, and L. J. Lauhon, Appl. Phys. Lett. **87**, 043111 (2005).